Conformational Analysis of Disaccharide Fragments of Blood Group Determinants in Solution by Molecular Modelling

F. BÍZIK and I. TVAROŠKA*

Institute of Chemistry, Slovak Academy of Sciences, SK-842 38 Bratislava

Received 4 September 1995

A detailed investigation has been undertaken on the conformational behaviour of seven disaccharide fragments from blood group determinants of Type 1 and Type 2, namely β-D-Gal-(1→3)-β-D-GlcNAc (*I*), β-D-Gal-(1→4)-β-D-GlcNAc (*II*), α-L-Fuc-(1→2)-β-D-Gal (*III*), α-L-Fuc-(1→3)-β-D-GlcNAc (*IV*), α-L-Fuc-(1→4)-β-D-GlcNAc (*V*), α-D-Gal-(1→3)-β-D-Gal (*VI*), and α-D-GalNAc-(1→3)-β-D-Gal (*VII*) in solution using molecular modelling methods. Two-dimensional rigid and adiabatic (Φ, Ψ) maps describing the energy as a function of rotation around corresponding glycosidic linkages were calculated by the RAMM molecular mechanics program which uses MM2(87) force field in conjunction with Monte Carlo simulation for a determination of the best side group orientations and with the evaluation of solvation effects. This approach predicted different conformational behaviour exhibited by these disaccharides. Whereas the rigid approach showed a very restricted motion about glycosidic linkages, the relaxed maps implied considerable increase of flexibility and several conformers were found for each of glycosidic linkages. Abundances of conformers appear to depend on the solvent. Comparison shows that the calculated data are in agreement with the available experimental data.

Several recent investigations have demonstrated that carbohydrates play diverse and crucial roles in a variety of biological systems. They are involved in blood clotting, lubrication, structural support, immunological protection, cell adhesion, hormone activity, and recognition events among others [1, 2]. The three-dimensional shape (conformation) adopted by these structures is crucial for their recognition by receptors and allows them to mediate the above events. Therefore, an understanding at the molecular level of the conformational behaviour of complex carbohydrates is of considerable importance for the understanding of their biological functions. In solution oligosaccharides usually exist as a mixture of several conformers and most of the experimental techniques give a time-averaged structure, the so-called virtual conformation [3]. As a result, a description of all conformers which exist in equilibrium is not accessible to direct experimental measurement and molecular modelling methods have to be used to yield a detailed geometrical model of oligosaccharides. Conformations of oligosaccharides in solution are determined by interactions between the sugar residues and between the oligosaccharide and solvent. The reliable prediction of the conformational preferences of an oligosaccharide requires a theoretical model that correctly describes all of these interactions [4, 5].

Carbohydrate structures related to blood group oligosaccharides are implicated in the recruitment of neutrophils at the site of inflammation by binding of endothelial leukocyte adhesion molecule [2]. In particular, it has been recently proposed that this process is mediated by the tetrasaccharide sialyl-Lewis X and the endothelial leukocyte adhesion molecule 1, glycoprotein of the E-selectin family [6]. Knowledge of the conformational behaviour of these molecules in solution is essential for understanding their function at the molecular level, evaluating its therapeutical potential, and designing the inhibitors or drugs. Determination of the three-dimensional structure of oligosaccharides brand as human blood determinants and of their disaccharide fragments in solution is currently the object of intense interest [7—21]. Some results have supported assumption of rigidity, mainly for tri- and tetraoligosaccharides. However, the conformational flexibility of disaccharides is still controversial.

Molecular modelling of these oligosaccharides involves several problems not addressed in previous studies. The most important are the effect of solvent on the conformational equilibrium and the orientations of all side groups. It has been shown that solvent, especially water, might considerably affect the equilibrium of conformers as well as the virtual conformation of oligosaccharides. The orientations of side groups present a very complex problem known in protein chemistry as multiple minima which is not sim-

* The author to whom the correspondence should be addressed.

ple to model. To evaluate the effect of these two factors on conformational behaviour of the blood group oligosaccharides and their sialylated derivatives in solution is of considerable interest. Therefore, in this study, the molecular mechanics method in conjunction with the Monte Carlo (MC) method for a determination of the best side group orientations and with the evaluation of solvation effects has been applied to study conformational behaviour of all disaccharide fragments from blood group determinants of Type 1 and Type 2 in solution. These include two so-called core disaccharides β-D-Gal-(1→3)-β-D-GlcNAc (*I*) and β-D-Gal-(1→4)-β-D-GlcNAc (*II*), and five other disaccharides: α-L-Fuc-(1→2)-β-D-Gal (*III*), α-L-Fuc-(1→3)-β-D-GlcNAc (*IV*), α-L-Fuc-(1→4)-β-D-GlcNAc (*V*), α-D-Gal-(1→3)-β-D-Gal (*VI*), and α-D-GalNAc-(1→3)-β-D-Gal (*VII*).

METHODS

Nomenclature

Representations of the seven disaccharides are shown in Scheme 1. The relative orientation of two monosaccharide residues is defined by torsion angles Φ(O-5′—C-1′—O-x—C-x) and Ψ(C-1′—O-x—C-x—C-$(x-1)$) or Φ^{H}(H-1′—C-1′—O-x—C-x) and Ψ^{H} (C-1′—O-x—C-x—H-x), where $x = 2, 3$ or 4.

Computational Methods

Conformational energy surfaces and minimum-energy conformations were calculated using the RAMM (RAndom walk Molecular Mechanics) program [22] that applies the MM2(87) force field [23]. The RAMM program uses the bond lengths, bond angles, and torsion angles as input parameters. These internal coordinates taken from diffraction data are used as starting values for the molecular mechanics (MM) calculations. The standard bond dipole approach with the value of the dielectric constant $\varepsilon = 1.5$ was used to describe electrostatic interactions. The minimum-energy conformation is calculated by minimizing the total energy with respect to the bond lengths, bond angles, and torsion angles using the nonderivative method of conjugate directions [24, 25].

Conformational energy of oligosaccharides depends strongly on the orientation of all the hydroxyl groups and other substituents in each ring as a result of their interactions. Consequently, the minimization of the energy usually leads to the structure which corresponds to the nearest local minimum of the initial structure [26]. To surmount this well-known multiple minimum problem and to find the best orientation of all rotatable groups for each oligosaccharide conformation we have employed the Monte Carlo method with Metropolis algorithm [27]. During this simulation, all exocyclic dihedral angles were treated as flex-

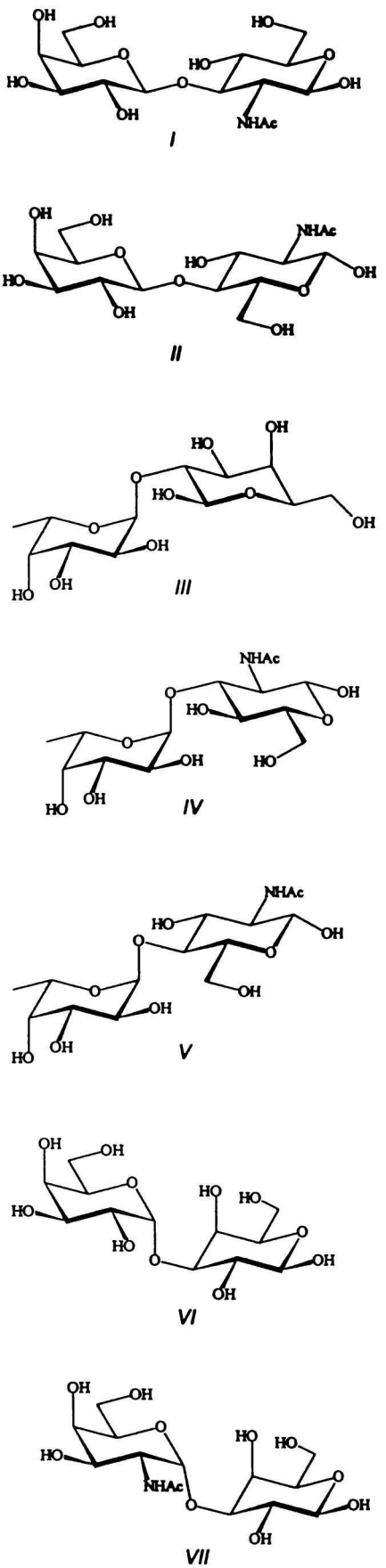

Scheme 1

ible. The algorithm comprises following steps. In the first, the energy of conformer in (Φ, Ψ) space is calculated. In the next one, the new orientations of all dihedral angles are altered by adding a random step and the energy of the new conformation state is calculated. Then the energy difference ΔE between the newly generated state and the previous state is calculated. If the new state has lower or equal energy in comparison with the old one, the state is always accepted, otherwise the Metropolis test is applied. After an adequate number of steps, the lowest energy state is selected and its energy minimized. It has turned out that 1500 steps were sufficient to find the lowest energy orientation of pendent groups in disaccharides *I*—*VII*.

Solvent Effect

In spite of the remarkable success of molecular simulations with computers in the past decades, it is not yet feasible to determine the solvation free energy for oligosaccharides by this method mainly due to the overwhelmingly large configurational space which solvent molecules can access for each of many conformational states of oligosaccharide. This uncomfortable situation prompted us to use the method based on the scaled particle theory [28]. This theory can give a rigorous description for liquid system consisting of hard spheres. The applicability of the method to a wider class of systems such as aqueous solution has already been demonstrated for the solubility of small nonpolar molecules in water [29]. The application of the modified version of this method to the solvation of saccharide conformers [30] showed a remarkable agreement with the experimentally observed effect of the solvent on the axial—equatorial equilibrium of 2-substituted tetrahydropyran derivatives [31, 32] and glucose [33]. The method was also successfully used to predict the effect of solvent on the conformational properties of various oligosaccharides [34]. In this procedure, the dissolution of the solute is decoupled into two steps by the thought experiment: *1.* creation of a cavity in solvent, which has the right size to accommodate the solute conformer, *2.* establishing the attractive interaction between the solvent and solute. The free energy of cavity formation can be estimated from the scaled particle theory formula. To calculate the contribution from the attractive interactions we assumed the Lennard—Jones type dispersion interactions and electrostatic interactions between the solvent and solute. The model and relevant equations have been described in detail in our previous papers [30, 35].

(Φ,Ψ) Maps

In preparing the rigid maps, the sugar rings of an oligosaccharide were treated as completely rigid entities that were rotated to specific values of the glycosidic angles Φ and Ψ, and the molecular energy in that conformation was then evaluated. Since the sugar rings are rigidly rotated around the glycosidic linkages, the resulting energy includes only van der Waals and electrostatic terms and intrinsic rotational energy of glycosidic linkage.

More physically realistic oligosaccharide (Φ, Ψ) maps are obtained when molecular geometry is "relaxed" by energy minimization to relieve strains at each value of Φ and Ψ on a regular 20° grid. In order to examine the influence of this internal flexibility on the available conformational space, adiabatic maps of compounds *I*—*VII* were constructed by allowing all the internal geometrical parameters to relax in the conjunction with the Monte Carlo procedure to find the lowest energy orientations of all rotatable groups. Thus, for compounds *I*—*VII*, a number of optimized parameters varied from 130 to 151. The accuracy of these geometrical parameters was 0.1 pm for bond lengths, 0.01° for bond angles, and 0.1° for torsion angles. The positions of the minima on the adiabatic (Φ, Ψ) maps were refined by consecutive complete minimization by including the torsion angles Φ and Ψ Subsequently, the solvation-energy maps for four solvents, namely 1,4-dioxane, methanol, dimethyl sulfoxide (DMSO), and water were calculated and superimposed on the vacuum adiabatic maps to give solvent-specific, adiabatic conformational energy (Φ, Ψ) maps.

Calculation of Mean Values for Carbon—Proton Coupling Constants

The interglycosidic one-bond and three-bond carbon—proton coupling constants ($^nJ_{C,H}$, n = 1 or 3) and distances between k and l protons r_{kl} were evaluated for every conformation of oligosaccharides. The heteronuclear one-bond and three-bond C,H coupling constants have been shown to depend besides other parameters also on the dihedral angle for the C—O—C—H segment *via* a Karplus-type relationship. The relation for vicinal couplings was established [36] from data obtained with the help of a series of rigid carbohydrates with known X-ray structures in the form

$$\{^3J_{C,H}\} = 5.7\cos^2\Theta - 0.6\cos\Theta + 0.5 \qquad (1)$$

Also the dependence of $^1J_{C,H}$ on the glycosidic torsion angles in oligosaccharides was described and characterized in the general form

$$\{^1J_{C,H}\} = A\cos 2\Theta + B\cos\Theta + C\sin 2\Theta + D\sin\Theta + E \qquad (2)$$

with different values of the constants A—E for the α- and β-anomer and for $^1J_{C,H}$ involving either the anomeric centre or corresponding to the aglycon C-x—H-x bond [37, 38]. Here, the dihedral angle Θ represents the corresponding glycosidic torsion angles Φ^H and Ψ^H.

Then these values were used to calculate the mean values of $^{n}J_{C,H}$ as ensemble averages over the whole map. At given temperature, the population of each conformer (P_i) depends upon its energy and is given by the Boltzmann distribution so that

$$P_i = \exp(-E_i(\Phi, \Psi)/RT)/Q \qquad (3)$$

where Q is the classical partition function

$$Q = \sum \exp[-E_i(\Phi, \Psi)/RT] \qquad (4)$$

The ensemble average values $\langle {}^{n}J_{C,H} \rangle$ are given as

$$\langle {}^{n}J_{C,H} \rangle = \sum P_i J_{C,H}(i) \qquad (5)$$

where $\langle {}^{n}J_{C,H} \rangle$ is distributed over the whole map.

RESULTS AND DISCUSSION

Conformational Energy Maps

The calculated relaxed energy surfaces (Φ, Ψ) for isolated disaccharides *I*—*VII* and their aqueous solutions are shown as potential energy contour maps in Figs. 1—7. The contours correspond to relative energies (ΔE/(kJ mol^{-1})) 5, 10, 15, 20, 30, 40, 50, and 60 above the lowest energy minimum of given disaccharide. The locations of minima are indicated on the conformational energy map for the isolated molecule. An overall shape of accessible energy surface to 60 kJ mol^{-1} is typical for this type of disaccharides and is dominated by steric interactions between contiguous monosaccharide residues and their functional groups. A comparison of adiabatic maps with the rigid ones (not shown) revealed significant differences in flexibility of the above molecules inferred from both types of maps. Whereas the rigid approach showed a very restricted motion about glycosidic linkages, the adiabatic maps implied considerable increase of flexibility and several conformers were found for each of glycosidic linkages. It can be seen from comparison of energy surfaces that the rotation about the bonds belonging to the torsion angles Φ^{H} is more restricted than that around Ψ^{H} angles. An exception are core disaccharides *I* and *II* where transition barriers are similar in both directions. Considerably restricted rotation can be observed for *IV*, where the available space given by the 60 kJ mol^{-1} energy contour is rather small. Within 60 kJ mol^{-1}, generally three low-energy regions have appeared on the relaxed energy maps. The main low-energy region is spreading about $\Phi^{H} = 0°$ and Ψ^{H} ranging from 0° to −60° and is characteristic of all analyzed molecules. The second region is centred about $\Phi^{H} = 0°$ and $\Psi^{H} = 180°$ The third low-energy area is situated in the domain about $\Phi^{H} = 180°$, $\Psi^{H} = 0°$ This region is not present on

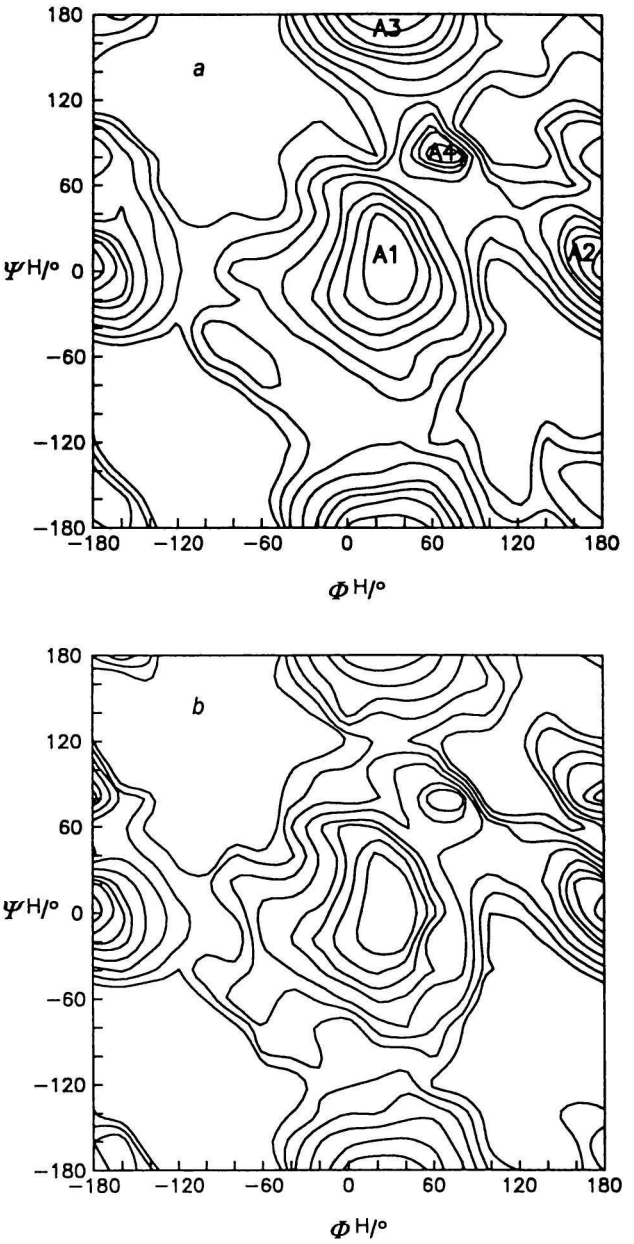

Fig. 1. Relaxed conformational energy maps for β-D-Gal-(1→3)-β-D-GlcNAc (*I*) in *a*) vacuum and *b*) water calculated using RAMM program with MM2(87) force field. Contours are drawn at ΔE/(kJ mol^{-1}) 5, 10, 15, 20, 30, 40, 50, and 60 above the lowest energy minimum of each map. Abbreviations designate minima referred to in the text and Table 1.

the energy surface within 60 kJ mol^{-1} for the isolated molecule of disaccharide *IV* There is also the next domain with local minima occurring approximately about $\Phi^{H} = 60°$, $\Psi^{H} = 60°$ for the molecules *I*, *IV, VI, VII.* This is not present for disaccharide *V*, but in this case the local minimum appeared about $\Phi^{H} = -60°$, $\Psi^{H} = -60°$ For molecule *III* the last mentioned region merged with the main low-energy region and created rather shallow surface. Additional

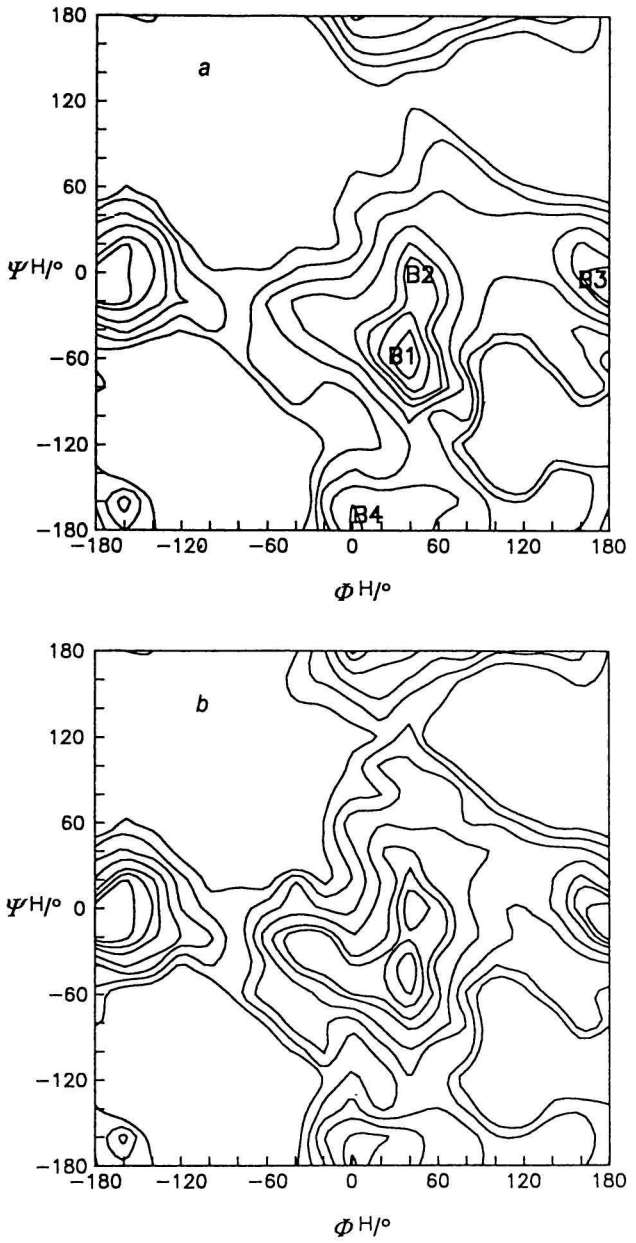

Fig. 2. Relaxed conformational energy maps for β-D-Gal-(1→4)-β-D-GlcNAc (*II*) in *a*) vacuum and *b*) water calculated using RAMM program with MM2(87) force field. Contours are drawn at $\Delta E/(\text{kJ mol}^{-1})$ 5, 10, 15, 20, 30, 40, 50, and 60 above the lowest energy minimum of each map. Abbreviations designate minima referred to in the text and Table 2.

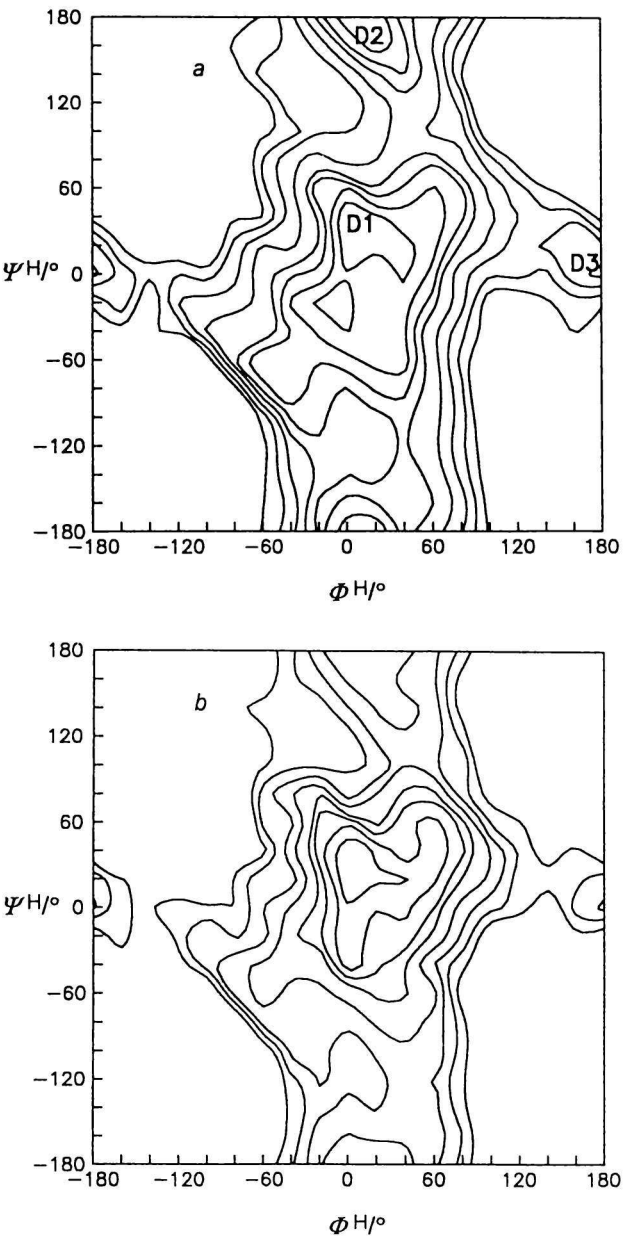

Fig. 3. Relaxed conformational energy maps for α-L-Fuc-(1→2)-β-D-Gal (*III*) in *a*) vacuum and *b*) water calculated using RAMM program with MM2(87) force field. Contours are drawn at $\Delta E/(\text{kJ mol}^{-1})$ 5, 10, 15, 20, 30, 40, 50, and 60 above the lowest energy minimum of each map. Abbreviations designate minima referred to in the text and Table 3.

minimum with high relative energies also appeared about $\Phi^{\text{H}} = -160°$ and $\Psi^{\text{H}} = -160°$ for β-linked disaccharides. Overall shape of the (Φ, Ψ) maps is similar to those calculated by the MM3 method [21] with understandable differences in details.

A comparison of the conformational energy maps for the same disaccharides in vacuum and aqueous solution shows only moderate changes of the overall shape of maps as a result of the solvent effect. However, significant alterations can be observed in energy barriers of transition between the local minima. This can be clearly recognized in Fig. 4 (disaccharide *IV*), where the energy barriers decreased in aqueous solution more than 20 kJ mol^{-1} Similarly, the changes in relative energies of local minima are observed, mainly at the minima having higher energy. This effect is especially large for *V* A complete geometry optimization including Φ, Ψ torsion angles starting from the

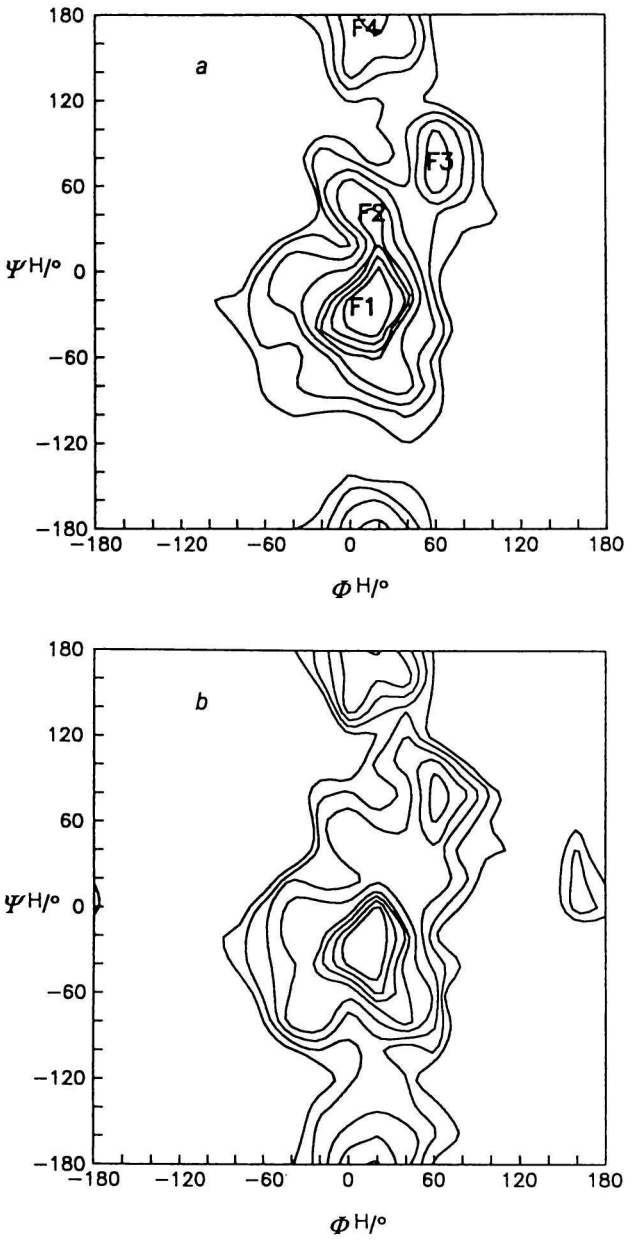

Fig. 4. Relaxed conformational energy maps for α-L-Fuc-(1→3)-β-D-GlcNAc (*IV*) in *a*) vacuum and *b*) water calculated using RAMM program with MM2(87) force field. Contours are drawn at ΔE/(kJ mol^{-1}) 5, 10, 15, 20, 30, 40, 50, and 60 above the lowest energy minimum of each map. Abbreviations designate minima referred to in the text and Table 4.

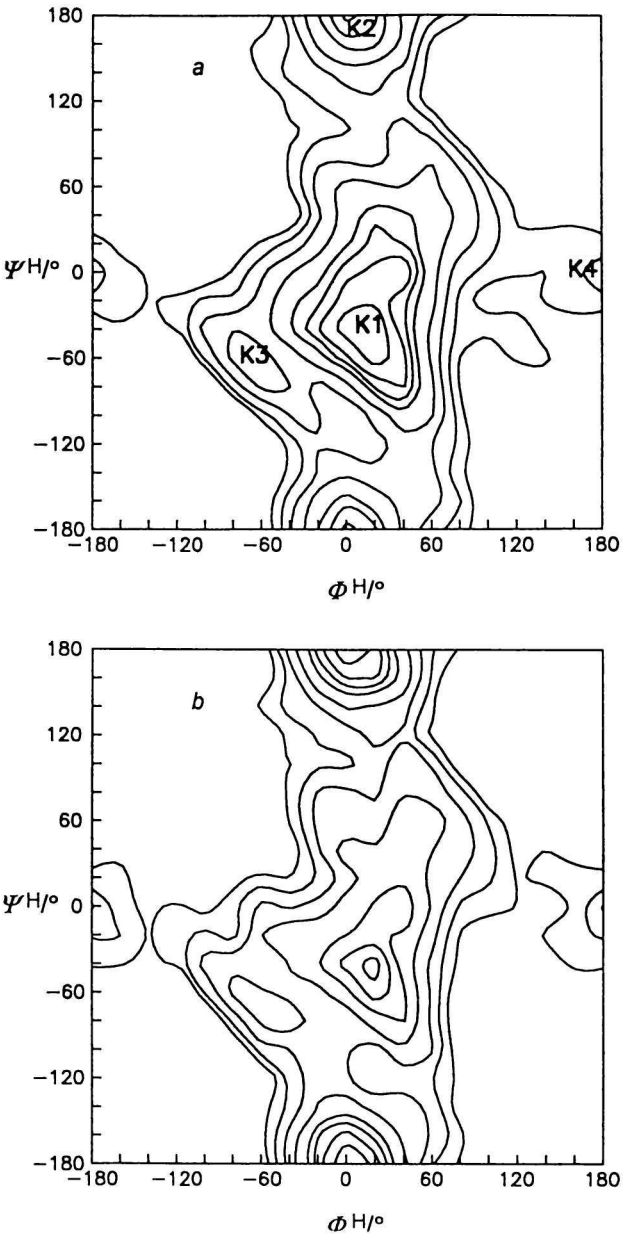

Fig. 5. Relaxed conformational energy maps for α-L-Fuc-(1→4)-β-D-GlcNAc (*V*) in *a*) vacuum and *b*) water calculated using RAMM program with MM2(87) force field. Contours are drawn at ΔE/(kJ mol^{-1}) 5, 10, 15, 20, 30, 40, 50, and 60 above the lowest energy minimum of each map. Abbreviations designate minima referred to in the text and Table 5.

low-energy regions led to the disclosure of four stable minima for the molecules *I*, *II*, *IV*—*VII* and three for *III*.

Description of the Minima

The geometrical characteristics and energies of predicted minima are listed in Tables 1—7 together with $^1J_{C,H}$ and $^3J_{C,H}$ carbon—proton coupling constants and $r_{H-1,H-x}$ proton—proton distances and dipole moments. Perhaps, it was not necessary to consider minima situated relatively high on the energy surface, but we did it in order to avoid casual loss of conformers in solution and to characterize the analyzed molecules in detail. For individual disaccharides, the differences in relative energies in vacuum between the lowest energy minimum and the second lowest energy conformer are between 2 kJ mol^{-1} and 16 kJ

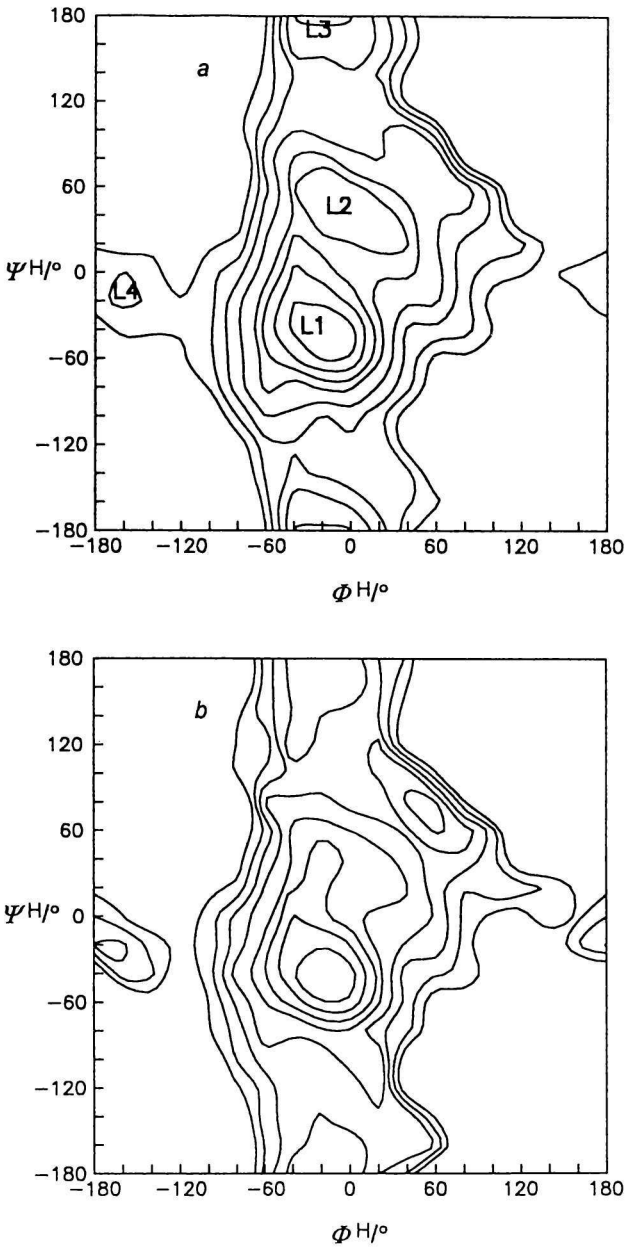

Fig. 6. Relaxed conformational energy maps for α-D-Gal-(1→3)-β-D-Gal (*VI*) in *a*) vacuum and *b*) water calculated using RAMM program with MM2(87) force field. Contours are drawn at ΔE/(kJ mol^{-1}) 5, 10, 15, 20, 30, 40, 50, and 60 above the lowest energy minimum of each map. Abbreviations designate minima referred to in the text and Table 6.

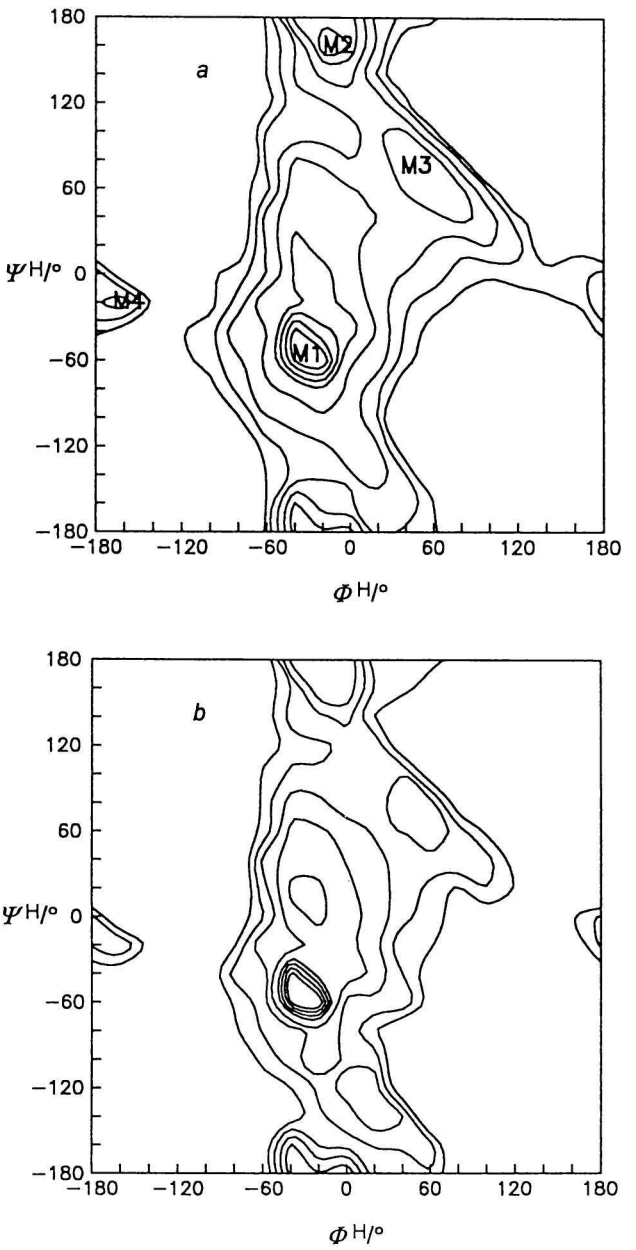

Fig. 7. Relaxed conformational energy maps for α-D-GalNAc-(1→3)-β-D-Gal (*VII*) in *a*) vacuum and *b*) water calculated using RAMM program with MM2(87) force field. Contours are drawn at ΔE/(kJ mol^{-1}) 5, 10, 15, 20, 30, 40, 50, and 60 above the lowest energy minimum of each map. Abbreviations designate minima referred to in the text and Table 7

mol^{-1} The comparison of positions of the lowest energy minima for individual disaccharides reveals that for all analyzed molecules the lowest energy minimum is located in the area previously referred as the main low-energy region. In these conformers aglycon carbon atom is in *gauche* orientation with respect to the ring oxygen in agreement with the exoanomeric effect [39].

The values of calculated one-bond coupling constants ($^1J_{C-1',H-1'}$) for α-linked disaccharides vary from 166.3 Hz for *V* (K3) to 174.1 Hz for *III* (D3). However, the range of $^1J_{C-1',H-1'}$ values of the lowest energy minima is only from 166.5 Hz for *V* (K1) to 167.0 Hz for *VI* (L1) or *VII* (M1). This is understandable because the torsion angles Φ^H of the lowest energy conformer for these molecules fluctuate from −27.9° for *VII* (M1) to 25.1° for *V* (K1). The $^1J_{C,H}$ values depending on Ψ angle are ranging from 143.8 Hz for *V* (K3) to 148.3 Hz. It is interesting that

Table 1. Numerical Values of Relative Energies ΔE/(kJ mol^{-1}), Torsion Angles Φ^H/°, Ψ^H/°, Φ/°, Ψ/°, Dipole Moments μ/D, Carbon—Proton Coupling Constants $^1J_{C,H}$/Hz, $^3J_{C,H}$/Hz and Proton—Proton Distances r_{ij}/pm Calculated for the Local Minima of β-D-Gal-(1→3)-β-D-GlcNAc (*I*)

	A1	A2	A3	A4
$\{\Delta E\}$	0.00	1.95	2.10	3.35
$\{\Phi^H\}$	31.3	179.2	18.6	75.9
$\{\Psi^H\}$	4.2	3.7	177.4	67.6
$\{\Phi\}$	−87.6	65.1	−100.5	−44.2
$\{\Psi\}$	−116.8	−115.1	61.5	−56.6
$\{\mu\}$	8.4	2.1	6.2	6.7
$\{^1J_{C-1',H-1'}\}$	159.5	165.5	159.2	159.5
$\{^1J_{C-3,H-3}\}$	144.1	144.1	146.1	144.1
$\{^3J_{C-3,H-1'}\}$	4.1	6.8	5.0	0.7
$\{^3J_{C-1',H-3}\}$	5.6	5.6	6.8	1.1
$\{r_{H-1',H-2}\}$	406.2	447.8	236.9	280.9
$\{r_{H-1',H-3}\}$	213.7	356.6	359.2	336.4
$\{r_{H-1',H-4}\}$	445.0	445.7	211.6	412.2
$\{r_{H-2',H-3}\}$	441.5	203.6	439.5	393.5
$\{r_{H-5',H-3}\}$	379.0	451.4	552.8	424.4

Table 2. Numerical Values of Relative Energies ΔE/(kJ mol^{-1}), Torsion Angles Φ^H/°, Ψ^H/°, Φ/°, Ψ/°, Dipole Moments μ/D, Carbon—Proton Coupling Constants $^1J_{C,H}$/Hz, $^3J_{C,H}$/Hz and Proton—Proton Distances r_{ij}/pm Calculated for the Local Minima of β-D-Gal-(1→4)-β-D-GlcNAc (*II*)

	B1	B2	B3	B4
$\{\Delta E\}$	0.00	9.48	10.63	15.06
$\{\Phi^H\}$	36.6	43.9	179.1	5.6
$\{\Psi^H\}$	−59.3	−6.5	−2.6	−174.2
$\{\Phi\}$	−85.0	−75.5	65.3	−111.4
$\{\Psi\}$	62.5	113.5	118.4	−59.5
$\{\mu\}$	3.8	4.1	5.0	5.6
$\{^1J_{C-1',H-1'}\}$	159.6	159.6	165.5	158.8
$\{^1J_{C-4,H-4}\}$	145.0	144.1	144.1	146.4
$\{^3J_{C-4,H-1'}\}$	3.7	3.0	6.8	5.5
$\{^3J_{C-1',H-4}\}$	1.7	5.5	5.6	6.7
$\{r_{H-1',H-3}\}$	356.5	442.5	440.9	205.6
$\{r_{H-1',H-4}\}$	237.0	222.0	357.9	357.6
$\{r_{H-1',H-5}\}$	448.0	417.0	451.8	244.3
$\{r_{H-2',H-4}\}$	448.9	442.7	215.8	436.2
$\{r_{H-5',H-4}\}$	438.4	372.5	454.6	558.3

Table 3. Numerical Values of Relative Energies ΔE/(kJ mol^{-1}), Torsion Angles Φ^H/°, Ψ^H/°, Φ/°, Ψ/°, Dipole Moments μ/D, Carbon—Proton Coupling Constants $^1J_{C,H}$/Hz, $^3J_{C,H}$/Hz and Proton—Proton Distances r_{ij}/pm Calculated for the Local Minima of α-L-Fuc-(1→2)-β-D-Gal (*III*)

	D1	D2	D3
$\{\Delta E\}$	0.00	4.08	23.92
$\{\Phi^H\}$	2.3	19.9	170.7
$\{\Psi^H\}$	40.0	173.1	11.8
$\{\Phi\}$	−112.9	−97.5	59.9
$\{\Psi\}$	158.0	−70.1	130.7
$\{\mu\}$	6.4	1.9	3.4
$\{^1J_{C-1',H-1'}\}$	166.8	166.5	174.1
$\{^1J_{C-2,H-2}\}$	144.3	148.3	144.6
$\{^3J_{C-2,H-1'}\}$	5.6	5.0	6.6
$\{^3J_{C-1',H-2}\}$	3.4	6.7	5.4
$\{r_{H-1',H-1}\}$	449.3	220.2	449.5
$\{r_{H-1',H-2}\}$	222.6	357.2	358.7
$\{r_{H-1',H-3}\}$	358.7	226.3	422.5
$\{r_{H-3',H-2}\}$	481.7	433.8	217.7
$\{r_{H-5',H-2}\}$	408.8	383.2	203.6

Table 4. Numerical Values of Relative Energies ΔE/(kJ mol^{-1}), Torsion Angles Φ^H/°, Ψ^H/°, Φ/°, Ψ/°, Dipole Moments μ/D, Carbon—Proton Coupling Constants $^1J_{C,H}$/Hz, $^3J_{C,H}$/Hz and Proton—Proton Distances r_{ij}/pm Calculated for the Local Minima of α-L-Fuc-(1→3)-β-D-GlcNAc (*IV*)

	F1	F2	F3	F4
$\{\Delta E\}$	0.00	15.75	18.28	23.99
$\{\Phi^H\}$	13.7	16.4	69.1	10.7
$\{\Psi^H\}$	−27.4	30.0	68.5	175.5
$\{\Phi\}$	−103.4	−100.3	−49.8	−106.4
$\{\Psi\}$	−143.9	−93.8	−54.5	58.7
$\{\mu\}$	5.6	2.8	5.4	4.4
$\{^1J_{C-1',H-1'}\}$	166.6	166.6	167.2	166.7
$\{^1J_{C-3,H-3}\}$	144.4	144.4	144.3	148.3
$\{^3J_{C-3,H-1'}\}$	5.3	5.1	1.0	5.4
$\{^3J_{C-1',H-3}\}$	4.4	4.2	1.0	6.7
$\{r_{H-1',H-2}\}$	438.9	374.6	271.4	220.5
$\{r_{H-1',H-3}\}$	210.4	222.0	330.7	357.0
$\{r_{H-1',H-4}\}$	398.9	445.0	409.4	215.3
$\{r_{H-1',H-5}\}$	437.7	481.3	548.5	475.8
$\{r_{H-2',H-3}\}$	425.3	451.5	489.4	526.6

one minimum with the value of $^1J_{C,H}$ = 148.3 Hz is presented for each compound from α-linked disaccharides. This results from the existence of only one local minimum with Ψ^H close to 180°. In β-linked disaccharides, lowest energy minima A1 and B1 for *I* and *II* are characterized by the value $^1J_{C-1',H-1'} \approx 159$ Hz due to a location of minima in the region of Φ^H torsion angles between 30° and 40° The values of one-bond coupling constants ($^1J_{C,H}$) related to torsion angle Ψ^H with values 4.2° (A1) and −59.3° (B1) are 144.1 Hz and 145.0 Hz, respectively.

A comparison of calculated $^3J_{C,H}$ values shows that three-bond coupling constants are more sensitive to small changes of torsion angles. This is a consequence of the angular dependence of $^3J_{C,H}$ values, which is the same for α- and β-linked disaccharides, as well as for both glycosidic torsion angles. These couplings vary for stable conformers from 0.7 Hz for *I* (A4) to 6.8 Hz for conformers with Ψ^H close to 180° The $^3J_{C,H}$ values of the lowest energy minima for in-

Table 5. Numerical Values of Relative Energies ΔE/(kJ mol^{-1}), Torsion Angles Φ^H/°, Ψ^H/°, Φ/°, Ψ/°, Dipole Moments μ/D, Carbon—Proton Coupling Constants $^1J_{C,H}$/Hz, $^3J_{C,H}$/Hz and Proton—Proton Distances r_{ij}/pm Calculated for the Local Minima of α-L-Fuc-(1→4)-β-D-GlcNAc (*V*)

	K1	K2	K3	K4
$\{\Delta E\}$	0.00	9.07	26.12	47.01
$\{\Phi^H\}$	25.1	7.5	−66.7	171.8
$\{\Psi^H\}$	−49.1	179.3	−61.3	1.2
$\{\Phi\}$	−93.0	−109.1	−179.8	61.3
$\{\Psi\}$	72.8	−65.1	62.4	121.3
$\{\mu\}$	1.8	5.9	3.1	7.3
$\{^1J_{C-1',H-1'}\}$	166.5	166.7	166.3	174.0
$\{^1J_{C-4,H-4}\}$	144.0	148.3	143.8	144.6
$\{^3J_{C-4,H-1'}\}$	4.6	5.5	1.1	6.7
$\{^3J_{C-1',H-4}\}$	2.5	6.8	1.5	5.6
$\{r_{H-1',H-1}\}$	563.6	373.8	540.0	631.5
$\{r_{H-1',H-2}\}$	439.2	471.0	464.9	587.1
$\{r_{H-1',H-3}\}$	362.4	211.9	283.3	438.6
$\{r_{H-1',H-4}\}$	225.8	356.4	324.1	359.9
$\{r_{H-1',H-5}\}$	443.8	226.6	428.0	434.9
$\{r_{H-2',H-4}\}$	440.4	525.4	387.6	410.2
$\{r_{H-3',H-4}\}$	473.2	433.2	252.3	223.0

Table 6. Numerical Values of Relative Energies ΔE/(kJ mol^{-1}), Torsion Angles Φ^H/°, Ψ^H/°, Φ/°, Ψ/°, Dipole Moments μ/D, Carbon—Proton Coupling Constants $^1J_{C,H}$/Hz, $^3J_{C,H}$/Hz and Proton—Proton Distances r_{ij}/pm Calculated for the Local Minima of α-D-Gal-(1→3)-β-D-Gal (*VI*)

	L1	L2	L3	L4
$\{\Delta E\}$	0.00	9.14	18.61	48.14
$\{\Phi^H\}$	−18.0	−17.4	−23.8	−176.2
$\{\Psi^H\}$	−43.6	53.6	−179.8	−20.8
$\{\Phi\}$	99.0	100.6	94.4	−66.0
$\{\Psi\}$	−162.2	−70.6	64.7	−139.7
$\{\mu\}$	3.9	1.7	3.4	7.0
$\{^1J_{C-1',H-1'}\}$	167.0	167.0	167.0	173.4
$\{^1J_{C-3,H-3}\}$	144.1	144.2	148.3	144.5
$\{^3J_{C-3,H-1'}\}$	5.1	5.1	4.7	6.8
$\{^3J_{C-1',H-3}\}$	3.0	2.1	6.8	4.9
$\{r_{H-1',H-2}\}$	442.2	352.4	211.2	437.4
$\{r_{H-1',H-3}\}$	237.2	230.6	358.5	360.0
$\{r_{H-1',H-4}\}$	225.5	419.7	363.0	399.1
$\{r_{H-5',H-3}\}$	375.0	448.8	384.6	218.1

dividual molecules are also in a relatively wide range, from 1.7 Hz for *II* (B1) to maximally 5.6 Hz for *I* and *III*.

Distribution of Conformers

Mole fractions of stable conformers calculated from energies for molecules in the isolated state and in four selected solvents (1,4-dioxane, methanol, dimethyl sulfoxide, water) at 300 K are given in Table 8. Rather large differences in relative energies for individual conformers are reflected in their populations. For all molecules, except *I*, the third and fourth minimum has always too high energy to be present in equilibrium mixture. In vacuum, there is characteristic occurrence of one dominant minimum. The most stable conformers are populated over 90 %, except for *III* (n(D1):n(D2) = 83:16). The molecule *I* appears to be more flexible than the remaining disaccharides and four conformers are present in equilibrium with vacuum populations n(A1):n(A2):n(A3):n(A4) = 46.6:21.3:20.0:12.1.

Table 7. Numerical Values of Relative Energies ΔE/(kJ mol^{-1}), Torsion Angles Φ^H/°, Ψ^H/°, Φ/°, Ψ/°, Dipole Moments μ/D, Carbon—Proton Coupling Constants $^1J_{C,H}$/Hz, $^3J_{C,H}$/Hz and Proton—Proton Distances r_{ij}/pm Calculated for the Local Minima of α-D-GalNAc-(1→3)-β-D-Gal (*VII*)

	M1	M2	M3	M4
$\{\Delta E\}$	0.00	8.64	20.36	34.88
$\{\Phi^H\}$	−27.9	−24.7	57.5	−168.2
$\{\Psi^H\}$	−46.5	178.1	68.2	−25.2
$\{\Phi\}$	89.3	92.6	168.8	−57.6
$\{\Psi\}$	−165.0	63.1	−57.0	−143.4
$\{\mu\}$	7.6	4.3	4.9	4.2
$\{^1J_{C-1',H-1'}\}$	167.0	167.0	166.7	172.8
$\{^1J_{C-3,H-3}\}$	144.0	148.3	144.3	144.4
$\{^3J_{C-3,H-1'}\}$	4.4	4.6	1.8	6.5
$\{^3J_{C-1',H-3}\}$	2.8	6.8	1.0	4.6
$\{r_{H-1',H-2}\}$	439.9	210.3	267.5	445.3
$\{r_{H-1',H-3}\}$	251.0	358.2	320.4	361.3
$\{r_{H-1',H-4}\}$	217.8	370.7	460.0	389.1
$\{r_{H-5',H-3}\}$	350.0	379.8	413.0	210.9

In solution, two different conformational behaviours are present among seven disaccharides. For five of them, disaccharides *III*—*VII*, one conformer dominates the other ones, representing more than 90 % in all solvents. For *III*, the distribution of D1 augments with increasing solvent polarity (93.46 % in 1,4-dioxane, 99.92 % in water) and D2 decreases (6.54 % in 1,4-dioxane, 0.08 % in water). An interesting change with solvent polarity is observed for *V* The population of K1 decreases with increasing solvent polarity (93.26 % in 1,4-dioxane, 6.12 % in water), whereas the population of K2 increases (6.74 % in 1,4-dioxane, 93.88 % in water). As a result, the occurrence of both conformers is reversed in water in comparison to vacuum. In methanol, the distribution of these two conformers is approximately equal (51.43 % of K1 and 48.57 % of K2). An analysis of solvation energy contributions revealed that the electrostatic term is responsible for this behaviour and the effect can be explained by considering dipole moments of these conformers. The conformer K2 with dipole moment 5.9 D is more stabilized in polar solvent than the vacuum-

Table 8. Calculated Mole Fractions of Stable Conformers for *I*—*VII* in Vacuum and Solution

	Vacuum	1,4-Dioxane	Methanol	DMSO	Water
		β-D-Gal-(1→3)-β-D-GlcNAc (*I*)			
n(A1)	46.56	66.30	88.95	86.07	71.32
n(A2)	21.27	11.22	4.07	4.06	25.30
n(A3)	20.03	12.42	2.53	4.36	0.54
n(A4)	12.14	10.06	4.45	5.51	2.84
		β-D-Gal-(1→4)-β-D-GlcNAc (*II*)			
n(B1)	96.26	94.73	85.27	89.84	48.23
n(B2)	2.15	2.87	7.46	5.13	30.14
n(B3)	1.36	2.04	6.26	4.28	19.83
n(B4)	0.23	0.36	1.01	0.75	1.80
		α-L-Fuc-(1→2)-β-D-Gal (*III*)			
n(D1)	83.66	93.46	99.38	98.68	99.92
n(D2)	16.33	6.54	0.62	1.32	0.08
n(D3)	0.01	0.00	0.00	0.00	0.00
		α-L-Fuc-(1→3)-β-D-GlcNAc (*IV*)			
n(F1)	99.74	99.83	99.82	99.86	99.14
n(F2)	0.18	0.09	0.02	0.02	0.01
n(F3)	0.07	0.07	0.14	0.11	0.63
n(F4)	0.01	0.01	-0.02	0.01	0.22
		α-L-Fuc-(1→4)-β-D-GlcNAc (*V*)			
n(K1)	97.43	93.26	51.43	72.33	6.12
n(K2)	2.57	6.74	48.57	27.67	93.88
n(K3)	0.00	0.00	0.00	0.00	0.00
n(K4)	0.00	0.00	0.00	0.00	0.00
		α-D-Gal-(1→3)-β-D-Gal (*VI*)			
n(L1)	97.44	98.29	99.47	99.25	99.86
n(L2)	2.50	1.66	0.51	0.72	0.13
n(L3)	0.06	0.04	0.02	0.03	0.00
n(L4)	0.00	0.00	0.00	0.00	0.00
		α-D-GalNAc-(1→3)-β-D-Gal (*VII*)			
n(M1)	96.94	98.90	99.91	99.80	99.99
n(M2)	3.04	1.09	0.09	0.20	0.01
n(M3)	0.03	0.01	0.00	0.00	0.00
n(M4)	0.00	0.00	0.00	0.00	0.00

dominant conformer K1 having dipole moment 1.8 D. Similarly, in polar solvents, the dipole moment 6.4 D is responsible for the increase of population of D1 in comparison to D2 which has dipole moment 1.9 D.

Two core disaccharides *I* and *II* behave in a different manner. The populations of these conformers are strongly influenced by solvent. However, in all solvents four conformers are present in equilibrium mixture. For *I*, the population of A1 conformer increases with the polarity of solvent from 47 % in vacuum to 71 % in water. On the contrary, the vacuum population of A3 (20 %) and A4 (12 %) decreases to the lowest value of 0.5 % and 2.8 %, respectively, in water. An interesting feature is observed for A2. The population of this conformer decreases from 21 % in vacuum to 4 % in methanol and then again increases to 25 % in water. For *II*, the conformation B1 dominates in 1,4-dioxane and has prevalent population also in methanol (85 %) and DMSO (89 %), but in water the population of B1 (48 %) is only slightly higher than that of B2 (30 %).

Comparison with Experimental Data and Previous Calculations

Molecular dynamic (MD) simulations of *I* predicted [16] that the most stable minimum is located in the region represented by conformer A1. During 120 ps simulation they observed several conformational transitions, all within this region. On the other hand, in recent MD investigations [20] of *I* a number of transitions between A1 and A2 minima were observed indicating that two minima have a similar energy region. It is noteworthy that the populations of conformers reported in this study are similar to those calculated in the present work. The calculated ensemble average values of geometrical parameters are listed in Table 9. Averaged glycosidic torsion angles $\langle \Phi^H \rangle = 35.8°$ and $\langle \Psi^H \rangle = 11.4°$ for *I* in vacuum and also in solution are slightly different from torsion angles for A1 conformer. Our calculated results for *I* are similar to those previously reported [16, 20]. Recently, $^3J_{C,H}$ were reported for trisaccharide Lewis a [40]. Though conformational behaviour of this compound might be different from *I*, the striking correspondence between experimental values $^3J_{C-1',H-3} = 5.0$ Hz and $^3J_{C-3,H-1'} = 3.8$—4.4 Hz and calculated averages 5.2 Hz and 4.7 Hz is observed. This suggests that substitution of core disaccharide *I* at the position 4 of galactose does not cause a significant change in the conformational behaviour of the trisaccharide Lewis a.

It can be seen from Table 9 that average glycosidic torsion angles for *II* in vacuum are $\langle \Phi^H \rangle = 39.3°$ and $\langle \Psi^H \rangle = -57.0°$ Also the changes of calculated parameters with solvent can be observed, although these are not so large. While the $\langle \Phi^H \rangle$ value is between 37° and 39° in all solvents, the average angle $\langle \Psi^H \rangle$ changed from −57° in vacuum to −33° in water. This change can be only difficult to observe from NOE, because interresidue distances between pairs of protons differ little. For this reason, a comparison of three-bond coupling constants in 1,4-dioxane and water is interesting. The average $\langle ^3J_{C-4,H-1'} \rangle$ value increased from 3.6 Hz in 1,4-dioxane to 4.2 Hz in water. Similarly, $\langle ^3J_{C-1',H-4} \rangle$ value increases from 2.1 Hz to 3.8 Hz going from 1,4-dioxane to water. The latter value can be compared with the value of 4.9 Hz observed for sialylated acetyllactosamine [41]. However, for Lewis X a higher value, $^3J_{C-4,H-1'} = 5.4$ Hz, was measured [41]. The grid search method and subsequent 120 ps MD simulation [17] predicted the average angles $\Phi = -46°$ and $\Psi = 111°$ This corresponds to the conformation shifted by 30° to the right (Φ^H scale), relative to B2. As it can be seen from Fig. 2, the energy has increasing tendency in this direction. From measurements of C—C coupling constants of Galβ1-4GlcNAc-hexanolamin [42], the angles $\Phi^H = 60°$ and $\Psi^H = 15°$ have been estimated. X-Ray data of crystal structure of *II* have been reported [43]. The conformation adopted by *II*

Table 9. Calculated Ensemble Averages of the Torsion Angles $\Phi^H/°$, $\Psi^H/°$, $\Phi/°$, $\Psi/°$ and Carbon—Proton Coupling Constants $^1J_{C,H}/Hz$, $^3J_{C,H}/Hz$

	Vacuum	1,4-Dioxane	Methanol	DMSO	Water
		β-D-Gal-(1→3)-β-D-GlcNAc (*I*)			
$\langle\{\Phi^H\}\rangle$	35.8	31.7	28.7	29.1	33.3
$\langle\{\Psi^H\}\rangle$	11.4	7.5	4.6	5.1	3.6
$\langle\{\Phi\}\rangle$	−84.0	−87.3	−89.8	−89.5	−85.9
$\langle\{\Psi\}\rangle$	−111.9	−114.2	−116.1	−115.8	−116.5
$\langle\{^1J_{C-1',H-1'}\}\rangle$	160.3	159.9	160.8	161.3	163.3
$\langle\{^1J_{C-3,H-3}\}\rangle$	144.7	144.5	145.1	145.5	146.4
$\langle\{^3J_{C-3,H-1'}\}\rangle$	4.5	4.4	4.4	4.3	4.7
$\langle\{^3J_{C-1',H-3}\}\rangle$	5.6	5.4	5.2	5.2	5.2
		β-D-Gal-(1→4)-β-D-GlcNAc (*II*)			
$\langle\{\Phi^H\}\rangle$	39.3	39.2	39.1	39.1	37.0
$\langle\{\Psi^H\}\rangle$	−57.0	−54.6	−45.8	−48.9	−33.2
$\langle\{\Phi\}\rangle$	−82.0	−82.0	−81.7	−81.8	−84.1
$\langle\{\Psi\}\rangle$	64.2	65.9	72.6	70.1	85.5
$\langle\{^1J_{C-1',H-1'}\}\rangle$	159.7	159.7	161.0	161.5	163.5
$\langle\{^1J_{C-4,H-4}\}\rangle$	145.0	144.9	145.6	146.1	146.7
$\langle\{^3J_{C-4,H-1'}\}\rangle$	3.5	3.6	3.7	3.6	4.2
$\langle\{^3J_{C-1',H-4}\}\rangle$	1.9	2.1	2.9	2.6	3.8
		α-L-Fuc-(1→2)-β-D-Gal (*III*)			
$\langle\{\Phi^H\}\rangle$	10.2	10.7	10.4	10.7	7.7
$\langle\{\Psi^H\}\rangle$	13.2	17.9	23.4	22.3	23.9
$\langle\{\Phi\}\rangle$	−105.9	−105.3	−105.3	−105.1	−107.5
$\langle\{\Psi\}\rangle$	133.1	137.3	142.1	141.2	142.2
$\langle\{^1J_{C-1',H-1'}\}\rangle$	166.7	166.8	168.0	168.5	169.8
$\langle\{^1J_{C-2,H-2}\}\rangle$	144.6	144.5	145.3	145.7	146.7
$\langle\{^3J_{C-2,H-1'}\}\rangle$	4.8	4.9	5.0	5.0	5.1
$\langle\{^3J_{C-1',H-2}\}\rangle$	4.2	4.1	4.1	4.0	4.2
		α-L-Fuc-(1→3)-β-D-GlcNAc (*IV*)			
$\langle\{\Phi^H\}\rangle$	13.6	13.5	13.3	13.4	13.2
$\langle\{\Psi^H\}\rangle$	−24.0	−23.5	−22.7	−22.8	−23.4
$\langle\{\Phi\}\rangle$	−103.5	−103.7	−103.8	−103.8	−103.9
$\langle\{\Psi\}\rangle$	−141.3	−141.0	−140.4	−140.5	−141.0
$\langle\{^1J_{H-1',C-1'}\}\rangle$	166.6	166.7	167.9	168.4	169.6
$\langle\{^1J_{C-3,H-3}\}\rangle$	144.4	144.4	145.3	145.7	146.7
$\langle\{^3J_{H-1',C-3}\}\rangle$	5.2	5.2	5.2	5.2	5.2
$\langle\{^3J_{C-1',H-3}\}\rangle$	4.5	4.5	4.6	4.6	4.5
		α-L-Fuc-(1→4)-β-D-GlcNAc (*V*)			
$\langle\{\Phi^H\}\rangle$	21.9	21.5	14.7	18.4	5.7
$\langle\{\Psi^H\}\rangle$	−40.5	−42.3	−98.3	−56.0	−177.5
$\langle\{\Phi\}\rangle$	−95.6	−96.0	−102.4	−98.9	−110.8
$\langle\{\Psi\}\rangle$	80.9	79.2	22.5	66.6	−62.0
$\langle\{^1J_{C-1',H-1'}\}\rangle$	166.5	166.6	167.9	168.4	169.8
$\langle\{^1J_{C-4,H-4}\}\rangle$	144.2	144.4	146.9	146.4	150.3
$\langle\{^3J_{C-4,H-1'}\}\rangle$	4.7	4.7	5.0	4.8	5.4
$\langle\{^3J_{C-1',H-4}\}\rangle$	3.3	3.4	4.8	4.1	6.5
		α-D-Gal-(1→3)-β-D-Gal (*VI*)			
$\langle\{\Phi^H\}\rangle$	−22.2	−22.1	−21.5	−21.8	−20.1
$\langle\{\Psi^H\}\rangle$	−37.4	−38.1	−39.1	−39.0	−38.6
$\langle\{\Phi\}\rangle$	95.1	95.2	95.8	95.5	97.2
$\langle\{\Psi\}\rangle$	−156.5	−157.3	−158.3	−158.2	−158.0
$\langle\{^1J_{C-1',H-1'}\}\rangle$	166.9	167.0	168.2	168.7	169.9
$\langle\{^1J_{C-3,H-3}\}\rangle$	144.1	144.2	145.1	145.5	146.4
$\{^3J_{C-3,H-1'}\}\rangle$	4.6	4.6	4.7	4.7	4.8
$\langle\{^3J_{C-1',H-3}\}\rangle$	3.3	3.3	3.3	3.3	3.4
		α-D-GalNAc-(1→3)-β-D-Gal (*VII*)			
$\langle\{\Phi^H\}\rangle$	−29.8	−29.7	−29.5	−29.6	−29.1
$\langle\{\Psi^H\}\rangle$	−56.0	−55.7	−55.5	−55.5	−55.4
$\langle\{\Phi\}\rangle$	87.3	87.3	87.6	87.5	87.9
$\langle\{\Psi\}\rangle$	−172.7	−172.3	−172.0	−172.1	−171.9
$\langle\{^1J_{C-1',H-1'}\}\rangle$	166.9	166.9	168.1	168.7	169.9
$\langle\{^1J_{C-3,H-3}\}\rangle$	144.0	143.9	144.8	145.2	146.2
$\langle\{^3J_{C-3,H-1'}\}\rangle$	4.2	4.2	4.2	4.2	4.3
$\langle\{^3J_{C-1',H-3}\}\rangle$	2.1	2.1	2.0	2.0	2.0

in crystal structure displays the values of $\Phi = -88.1°$ and $\Psi = 97.8°$

The calculated values of ensemble average geometrical parameters for *III* are given in Table 9. Average values of torsion angles $\langle \Phi^H \rangle$ and $\langle \Psi^H \rangle$ demonstrate that solution conformations do not change significantly in different solvents. In water we have obtained average angles $\langle \Phi^H \rangle = 7.7°$ and $\langle \Psi^H \rangle = 23.9°$ MD simulations [16] of *III* showed several transitions which could correspond to the motion within rather shallow main low-energy region on the conformational energy map with the minimum-energy structure at $\Phi = -72°$ and $\Psi = 126°$ This Φ angle is shifted approximately by 30° in comparison to our average value of Φ angle. The similar deviation observed for *I* and *III* suggests that the observed discrepancy is likely due to different force fields applied.

Calculated average values of glycosidic torsion angles for *IV* in aqueous solution ($\langle \Phi^H \rangle = 13.2°$ and $\langle \Psi^H \rangle = -23.4°$) are in fact the same as those for other solvents, and demonstrate that solvent has a negligible effect on the preferred conformation. The comparison of calculated parameters for the lowest energy conformer F1 with ensemble averages shows that these are fairly similar and indicates considerable rigidity of this disaccharide.

The ensemble average values for *V* show how different can be the behaviour of molecules in solution with different type of glycosidic linkage. While for (1→3) linkage (disaccharide *IV*), the same dominant structure has been found in all reported solvents, conformational equilibrium about the (1→4) linkage shows a strong solvent dependence. If we consider only solution conformations, the most pronounced differences were observed for 1,4-dioxane ($\langle \Phi^H \rangle = 21.5°$, $\langle \Psi^H \rangle = -42.3°$) and aqueous solution ($\langle \Phi^H \rangle = 5.7°$, $\langle \Psi^H \rangle = -177.5°$). The comparison of averages with geometrical parameters for conformers K1 and K2 (Table 5) reveals that the main contribution to average values in 1,4-dioxane solution comes from conformer K1, while for aqueous solution it is K2. It is noteworthy that for methanol solution, the average glycosidic torsion angles ($\langle \Phi^H \rangle = 14.7°$, $\langle \Psi^H \rangle = -98.3°$) correspond to the virtual conformation located on the barrier. On the conformational energy map for methanol (not shown) this conformer has relative energy 32 kJ mol^{-1} above the lowest energy minimum. With regard to this conformational fluctuation, the influence of solvent on other calculated parameters is expected. The $\langle {}^3J_{C-4,H-1'} \rangle$ value increased from 4.7 Hz in 1,4-dioxane to 5.4 Hz in water. Even larger difference has been found for $\langle {}^3J_{C-1',H-4} \rangle$, the range is from 3.4 Hz (1,4-dioxane) to 6.5 Hz (water). Calculated values in water are about 1 Hz higher than the experimental values for Lewis a [40]. Previous investigation [17] suggested that considerable amount of flexibility exists about the glycosidic linkage of the disaccharide *V* The most stable conformation was found at $\Phi = -75°$ and $\Psi = 110°$ A comparison with our lowest energy conformer shows that similarly as in some previous cases, there is a deviation over 30° at Ψ and also about 20° at Φ angle. Moreover, the conformer marked as K2 on our conformational map although presented also on their contour map was not considered in that study. In fact, the conformer K2 is less populated in vacuum, but as it was shown, the including of solvent effect has a considerable impact on the preferred conformation.

The comparison of the data for *VI* and *VII* shows that substitution of the hydroxyl group by acetamido group has only little influence on the calculated average parameters. In aqueous solution, the average torsion angles $\langle \Phi^H \rangle$ and $\langle \Psi^H \rangle$ of *VI* are −20.1° and −38.6°, respectively. The same angles of disaccharide *VII* ($\langle \Phi^H \rangle = -29.1°$, $\langle \Psi^H \rangle = -55.4°$) are 9° less at $\langle \Phi^H \rangle$ and 17° at $\langle \Psi^H \rangle$. In vacuum and other reported solvents, the glycosidic torsion angles are very similar and imply that the solvents have nondetectable influence on conformations of these two disaccharides. The average three-bond coupling constant $\langle {}^3J_{C-3,H-1'} \rangle = 4.3$ Hz for *VII* is only by 0.5 Hz less than that for *VI* ($\langle {}^3J_{C-3,H-1'} \rangle = 4.8$ Hz). A little greater difference was found for $\langle {}^3J_{C-1',H-3} \rangle$, where the value for *VII* ($\langle {}^3J_{C-1',H-3} \rangle = 2.0$ Hz) is about 1.4 Hz lower than that for *VI* ($\langle {}^3J_{C-1',H-3} \rangle = 3.4$ Hz). Similarly as in the previous cases, molecular dynamics of *VI* and *VII* predicted for both compounds the common lowest energy conformation at $\Phi = 60°$ and $\Psi = -160°$

The results of molecular mechanics calculations of the conformational energy surfaces for seven disaccharide fragments of blood group determinants of Type 1 and Type 2 lead to the following conclusions.

The procedures used in this study allowed us to investigate thoroughly the conformational behaviour of blood group disaccharides and to estimate the influence of solvent effect. In addition to the lowest energy minima several secondary minima were identified on the (Φ, Ψ) surface for these disaccharides. These results provide a basis for further investigations of blood group oligosaccharides and the possible mode of interaction of such molecules with receptors.

Comparison of the rigid and relaxed energy maps clearly demonstrates that optimization of the geometry and orientation of pendent groups have a significant influence on the predicted conformational flexibility of these disaccharides.

There are four possible low-energy domains for the core disaccharides (*I* and *II*) where all minima appear. These minima are present in equilibrium for all solvents and demonstrate significant flexibility of these disaccharides. Therefore, the measured NMR values describe averaged, virtual conformation.

For α-linked disaccharides (*III*—*VII*) only one dominant conformer was found and it appears that solvent has a negligible effect on the conformation of these disaccharides. Therefore, glycosidic linkages in these disaccharides can be assumed as relatively

rigid. An exception is α-L-Fuc-(1→4)-β-D-GlcNAc (*V*) where two regions on (Φ, Ψ) maps appeared populated, the first is dominant in nonpolar solvents and the second one in water.

Acknowledgements. This investigation was supported by the grant No. 2/1235/94 from the Slovak Grant Agency for Science.

REFERENCES

1. Ruud, P., *GlycoNews*, 1 (1993).
2. Varki, A., *Glycobiology 3*, 97 (1993).
3. Jardetzky, O., *Biochem. Biophys. Acta 621*, 227 (1980).
4. Brady, J. W., *Curr. Opin. Struct. Biol. 1*, 711 (1991).
5. Carver, J. P., *Curr. Opin. Struct. Biol. 1*, 716 (1991).
6. Phillips, M. L., Nudelman, E., Gaeta, C. A., Perez, M., Singhai, A. K., Hakomori, S. I., and Paulson, J. C., *Science 250*, 1130 (1990).
7. Lemieux, R. U., Bock, K., Dalbaere, L. T. J., Koto, S., and Rao, V. S., *Can. J. Chem. 58*, 631 (1980).
8. Biswas, M. and Rao, V. S. R., *Biopolymers 19*, 1555 (1980).
9. Lemieux, R. U., Wong, T. C., and Thogersen, H., *Can. J. Chem. 60*, 81 (1982).
10. Thogersen, H., Lemieux, R. U., Bock, K., and Meyer, B., *Can. J. Chem. 60*, 44 (1982).
11. Rosevar, P. R., Nunez, H. A., and Barker, R., *Biochemistry 21*, 1421 (1982).
12. Biswas, M. and Rao, V. S. R., *Carbohydr. Polymer 2*, 205 (1982).
13. Bock, K., Arnap, J., and Longren, J., *Eur. J. Biochem. 129*, 171 (1982).
14. Rao, B. N. N., Dua, V. K., and Bush, C. A., *Biopolymers 24*, 2207 (1985).
15. Bush, C. A., Yan, Z.-Y., and Rao, B. N. N., *J. Am. Chem. Soc. 108*, 6168 (1986).
16. Yan, Z.-Y. and Bush, C. A., *Biopolymers 29*, 799 (1990).
17. Mukhopadhyay, C. and Bush, C. A., *Biopolymers 31*, 1737 (1991).
18. Bush, C. A. and Cagas, P., *Adv. Biophys. Chem. 2*, 149 (1992).
19. Renouf, D. V. and Hounsell, E. F., *Int. J. Biol. Macromol. 15*, 37 (1993).
20. Toma, L., Ciuffreda, P., Colombo, D., Ronchetti, F., Lay, L., and Panza, L., *Helv. Chim. Acta 77*, 668 (1994).
21. Imberty, A., Mikros, E., Koca, J., Mollicone, R., Oriol, R., and Perez, S., *Glycoconjugate J.*, in press.
22. Kožár, T., Petrák, F., Gálová, Z., and Tvaroška, I., *Carbohydr. Res. 204*, 27 (1990).
23. Burkert, U. and Allinger, N. L., *Molecular Mechanics*. American Chemical Society, Washington, D.C., 1982.
24. Powell, M. J. D., *Comput. J. 7*, 155 (1964).
25. Zangwill, W. I., *Comput. J. 10*, 293 (1967).
26. Brady, J. W., *Adv. Biophys. Chem. 1*, 155 (1990).
27. Metropolis, N., Rosenbluth, A. W., Rosenbluth, M. M., Teller, A. H., and Teller, E., *J. Phys. Chem. 21*, 1087 (1953).
28. Reiss, H., Frisch, H. L., and Lebowitz, J. L., *J. Chem. Phys. 31*, 369 (1959).
29. Pierotti, R. A., *Chem. Rev. 76*, 717 (1976).
30. Tvaroška, I. and Kožár, T., *J. Am. Chem. Soc. 102*, 6929 (1980).
31. Tvaroška, I. and Carver, J. P., *J. Phys. Chem. 98*, 6452 (1994).
32. Tvaroška, I. and Carver, J. P., *J. Phys. Chem. 98*, 9477 (1994).
33. Tvaroška, I. and Kožár, T., *Theor. Chim. Acta 70*, 99 (1986).
34. Tvaroška, I., *Curr. Opin. Struct. Biol. 2*, 661 (1992).
35. Tvaroška, I., *Biopolymers 21*, 1887 (1982).
36. Tvaroška, I., Hricovíni, M., and Petráková, E., *Carbohydr. Res. 189*, 359 (1989).
37. Tvaroška, I. and Taravel, F. R., *Carbohydr. Res. 221*, 83 (1991).
38. Tvaroška, I. and Taravel, F. R., *J. Biomol. NMR 2*, 421 (1991).
39. Tvaroška, I. and Bleha, T., *Adv. Carbohydr. Chem. Biochem. 47*, 45 (1989).
40. Kogelberg, H. and Rutherford, T. J., *Glycobiology 4*, 49 (1994).
41. Ichikawa, Y., Lin, Y. Y., Dumas, D. P., Shen, G. J., Garcia-Junceda, E., Williams, M. A., Bayer, R., Ketcham, C., Walker, L. E., Paulson, J. C., and Wong, C. H., *J. Am. Chem. Soc. 114*, 9283 (1992).
42. Longchambon, F., Ohanessian, J., Gillier-Pandraud, H., Duchet, D., Jacquinet, J.-C., and Sinay, P., *Acta Crystallogr., B 37*, 601 (1981).
43. Nunez, H. A. and Baker, R., *Biochemistry 19*, 489 (1980).

Translated by the authors